*Netsu Sokutei* **27** (3) 118-127

論 文

# Single Crystal X-ray Diffraction and Low Temperature Calorimetric Studies of the Thiourea-hexachloroethane Adduct*

Yoshiyuki Mizutani, Hatsue Tamura, Takasuke Matsuo**,
Hiroshi Suga#, and Gen-etsu Matsubayashi

(Received April 14, 2000; Accepted May 22, 2000)

The thiourea hexachloroethane adduct has been studied by single crystal X-ray diffraction and low temperature calorimetry. The guest molecules are disordered in three orientations in the adduct channel. The thermal properties are described consistently by a model involving the orientational disorder of the guest molecules and their ordering in a phase transition at 96 K. A small degree of disorder persists to lower temperatures and becomes frozen into an immobile state below a glass transition at 59 K.

## 1. Introduction

In clathrate compounds, the guest molecules are separated from each other by the wall of the host molecules. Because of this general structural principle, interaction between the guest molecules is relatively weak and plays only a secondary role in determining the properties of the compound. It has been customary to discuss the clathrate system only in terms of the host-guest interaction. However, in certain situations the guest-guest interaction reveals itself in a striking way at low temperature.[1-9] In the present paper we report X-ray diffraction and low temperature calorimetric studies on the thiourea-hexachloroethane clathrate compound where such interaction gives rise to a phase transition and is responsible, along with the host-guest interaction, to a glass transition. As to the terminology, clathrate compounds, inclusion compounds and adducts are used more or less interchangeably. We follow the general usage by describing the thiourea compounds as adducts.

The generic formula of the compound is $(\text{thiourea})_3$-G where thiourea is $(NH_2)_2CS$ and G a guest molecule. The guest molecules are cyclic and branched aliphatic hydrocarbons or halo-substituted methanes and ethanes.[10,11] Structurally the host lattice encloses the guest molecules in the channels similar in shape to those of a honeycomb. The honeycomb structure of thiourea appears to be unstable by itself. Attempts to prepare an empty host lattice or non-stoichiometric adducts in which some of the channel-cavities are not occupied by guest molecules have been unsuccessful.

## 2. Experiment

### 2.1 Sample Preparation

The hexachloroethane thiourea adduct was prepared from an acetic acid solution.[11] The starting materials (thiourea and hexachloroethane) were dissolved in 3:1 molar ratio in acetic acid at 90 ℃. The adduct crystallized out from the solution kept overnight at 25 ℃. The crystal was separated from the solution and stored in a desiccator together with KOH pellets.

Single crystals suitable for X-ray diffraction were grown by evaporation of the solution over KOH pellets in a closed desiccator.

---

* Contribution No.24 from the Molecular Thermodynamics Research Center.

** Author for correspondence

# Present Address: Research Institute for Science and Technology, Kinki Univ., Higashi Osaka 577-8502, Japan

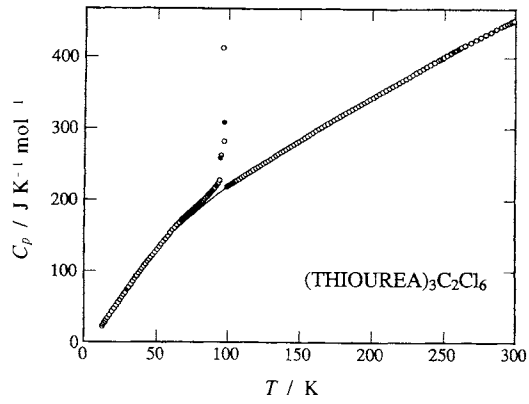


**Fig.1** Molar heat capacity of thiourea adduct $[(NH_2)_2CS]_3C_2Cl_6$.

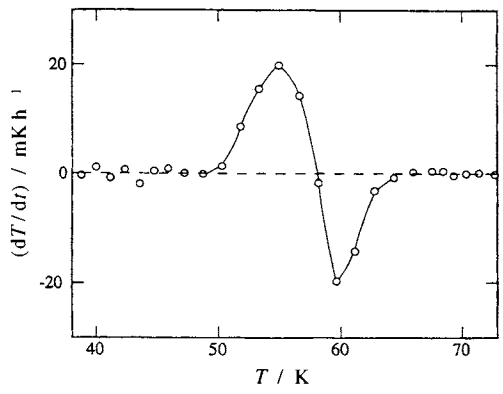


**Fig.2** Temperature drift rate recorded during the measurement of the heat capacity of thiourea adduct $[(NH_2)_2CS]_3C_2Cl_6$.

The composition of the clathrate compound was determined by elemental analysis. C 12.99 %, H 2.64 %, N 18.07 %, S 20.58 %, Cl 46.00 %. Calculated values based on the 3:1 stoichiometry are C 12.91 %, H 2.60 %, N18.07 %, S 20.68 % and Cl 45.74 %.

### 2.2 Heat Capacity Measurement

The calorimeter used for the measurement has been described elsewhere.[12] Inaccuracy of the measurement has been estimated to be less than 0.3 % above 30 K. Scattering of the data points about the smoothed curve was less than 0.1 %. The sample (4.1535 g) was sealed in the sample cell of the calorimeter in a dry helium atmosphere and mounted in the calorimetric cryostat.

The heat capacity was measured between 12 and 300 K at temperature steps of 2 to 3 K in the normal region. A phase transition was found at 96 K. The measurement was repeated in the transition region at smaller temperature intervals. The enthalpy of transition was absorbed by the crystal quasi-isothermally at the transition temperature. The heat capacity is shown in **Fig.1** for the entire temperature region. The curve is smooth except at two temperatures. One is the transition point 96 K and the other a step-like anomaly at 59 K. The latter anomaly, not very evident in **Fig.1**, was more clearly shown in the temperature drift rate. As the temperature approached 50 K from below, the sample warmed by itself spontaneously. The heat evolution occurred steadily during the intervals for the temperature measurement of each cycle of the heat capacity determination. Obviously it occurred during the heating as well, only to be masked by much stronger temperature rise due to the calorimeter Joule heating. The spontaneous heating occurred at four consecutive temperature measurements up to 58 K. At this temperature it was taken over by spontaneous cooling that occurred for a certain period of time after the heating current was turned off. **Fig.2** shows the temperature drift rate taken at 5 min after the heating interval. This type of drift behavior (i.e., first exothermic and then endothermic drift) occurs in a glass around its glass transition region. It can also occur in a crystal that retains disorder at low temperature.[13] The relaxation effect is discussed below in more detail. Numerical values of the heat capacity are collected in **Table 1**. The series numbers (3-10) describing the time order of experiment are also given. The data were reproducible as the different series of measurement shows.

### 2.3 X-Ray Diffraction

A single crystal of dimensions $0.6 \times 0.5 \times 0.4$ mm was selected for data collection. The cell dimension and diffraction intensities were measured at 233 K using a Rigaku four circle diffractometer AFC-5R equipped with a Rigaku low temperature device (liquid nitrogen as the coolant) and graphite-monochromatized Mo $K\alpha$ radiation. Accurate cell dimensions were refined using 25 reflections in the range $49.80^\circ \leqq 2\theta \leqq 49.93^\circ$. In total 1995 reflections were collected by the $\omega$-$2\theta$ scan mode up to $2\theta = 60^\circ$. Since the intensities of three standard reflections monitored at every 100 reflections decreased only by 0.7 % on the average, no correction

**Table 1** Experimental molar heat capacities of (thiourea)$_3C_2Cl_6$ adduct.

| $T$/K | $C_p/R$ | Ser. | $T$/K | $C_p/R$ | Ser. | $T$/K | $C_p/R$ | Ser. | $T$/K | $C_p/R$ | Ser. |
|---|---|---|---|---|---|---|---|---|---|---|---|
| 12.73 | 2.71 | 4 | 72.06 | 21.62 | 5 | 122.75 | 29.97 | 6 | 221.02 | 44.24 | 8 |
| 13.51 | 3.00 | 4 | 72.75 | 21.78 | 5 | 124.50 | 30.24 | 6 | 223.37 | 44.55 | 8 |
| 14.25 | 3.28 | 4 | 73.45 | 21.94 | 5 | 126.25 | 30.50 | 6 | 225.78 | 44.90 | 8 |
| 15.02 | 3.56 | 4 | 74.86 | 22.25 | 5 | 127.99 | 30.77 | 6 | 228.17 | 45.22 | 8 |
| 15.79 | 3.85 | 4 | 75.58 | 22.42 | 5 | 129.73 | 31.02 | 6 | 230.56 | 45.57 | 8 |
| 16.55 | 4.13 | 4 | 76.36 | 22.60 | 5 | 131.47 | 31.27 | 6 | 232.95 | 45.88 | 8 |
| 17.78 | 4.58 | 4 | 78.04 | 22.98 | 5 | 133.23 | 31.56 | 6 | 235.34 | 46.22 | 8 |
| 19.41 | 5.18 | 4 | 78.89 | 23.18 | 5 | 135.02 | 31.82 | 6 | 237.44 | 46.53 | 10 |
| 20.88 | 5.73 | 4 | 79.74 | 23.37 | 5 | 136.81 | 32.08 | 6 | 237.72 | 46.58 | 8 |
| 22.25 | 6.23 | 4 | 80.59 | 23.57 | 5 | 138.60 | 32.35 | 6 | 240.16 | 46.95 | 8 |
| 23.57 | 6.71 | 4 | 81.50 | 23.80 | 5 | 140.38 | 32.61 | 6 | 240.17 | 46.91 | 10 |
| 24.87 | 7.17 | 4 | 82.47 | 23.99 | 5 | 142.15 | 32.88 | 6 | 242.56 | 47.31 | 9 |
| 26.10 | 7.61 | 4 | 83.44 | 24.23 | 5 | 143.96 | 33.16 | 6 | 242.98 | 47.30 | 10 |
| 27.30 | 8.04 | 4 | 84.41 | 24.49 | 5 | 145.79 | 33.44 | 6 | 245.85 | 47.69 | 10 |
| 28.49 | 8.45 | 4 | 85.38 | 24.72 | 5 | 147.62 | 33.70 | 6 | 247.20 | 47.88 | 9 |
| 29.63 | 8.98 | 4 | 86.23 | 24.94 | 3 | 149.51 | 33.98 | 7 | 248.73 | 48.01 | 10 |
| 30.27 | 9.16 | 4 | 86.36 | 24.98 | 5 | 151.44 | 34.28 | 7 | 249.53 | 48.18 | 9 |
| 30.78 | 9.30 | 4 | 87.38 | 25.23 | 5 | 153.37 | 34.57 | 7 | 251.67 | 48.51 | 10 |
| 32.22 | 9.83 | 4 | 88.46 | 25.53 | 5 | 155.30 | 34.85 | 7 | 251.92 | 48.53 | 9 |
| 33.54 | 10.29 | 4 | 88.62 | 25.57 | 3 | 157.28 | 35.14 | 7 | 254.38 | 48.85 | 10 |
| 34.88 | 10.78 | 4 | 89.53 | 25.83 | 5 | 159.30 | 35.42 | 7 | 254.69 | 48.89 | 9 |
| 35.68 | 11.16 | 4 | 90.60 | 26.14 | 5 | 161.32 | 35.73 | 7 | 256.53 | 49.17 | 9 |
| 36.24 | 11.26 | 4 | 91.56 | 26.48 | 3 | 163.33 | 36.01 | 7 | 257.78 | 49.30 | 10 |
| 37.54 | 11.69 | 4 | 91.67 | 26.50 | 5 | 165.35 | 36.27 | 7 | 258.31 | 49.41 | 9 |
| 38.79 | 12.11 | 4 | 92.74 | 26.88 | 5 | 167.36 | 36.59 | 7 | 260.02 | 49.64 | 9 |
| 40.00 | 12.51 | 4 | 93.86 | 27.45 | 5 | 169.41 | 36.89 | 7 | 260.94 | 49.72 | 10 |
| 41.18 | 12.88 | 4 | 94.34 | 31.16 | 3 | 171.51 | 37.20 | 7 | 261.74 | 49.89 | 9 |
| 42.37 | 13.27 | 4 | 94.98 | 31.62 | 5 | 173.60 | 37.51 | 7 | 264.46 | 50.18 | 10 |
| 43.59 | 13.65 | 4 | 95.97 | 49.66 | 5 | 175.69 | 37.81 | 7 | 268.34 | 50.68 | 10 |
| 44.78 | 14.02 | 4 | 96.88 | 37.10 | 3 | 177.77 | 38.13 | 7 | 271.99 | 51.16 | 10 |
| 45.94 | 14.40 | 4 | 96.94 | 33.95 | 5 | 179.86 | 38.40 | 7 | 275.41 | 51.61 | 10 |
| 47.25 | 14.78 | 4 | 98.06 | 27.79 | 5 | 181.98 | 38.72 | 7 | 278.92 | 52.04 | 10 |
| 48.77 | 15.24 | 4 | 99.24 | 26.33 | 5 | 184.15 | 39.04 | 7 | 282.51 | 52.51 | 10 |
| 50.30 | 15.70 | 4 | 99.48 | 26.44 | 3 | 186.32 | 39.34 | 7 | 286.18 | 53.04 | 10 |
| 51.83 | 16.14 | 4 | 100.49 | 26.52 | 5 | 188.48 | 39.67 | 7 | 289.92 | 53.48 | 9 |
| 53.36 | 16.57 | 4 | 101.78 | 26.72 | 5 | 190.54 | 39.95 | 7 | 289.93 | 53.47 | 10 |
| 55.00 | 17.02 | 4 | 102.24 | 26.80 | 3 | 192.51 | 40.24 | 8 | 291.93 | 53.70 | 9 |
| 56.65 | 17.49 | 4 | 103.07 | 26.93 | 5 | 194.46 | 40.52 | 8 | 293.94 | 53.91 | 9 |
| 58.18 | 17.93 | 4 | 104.36 | 27.13 | 6 | 196.41 | 40.78 | 8 | 295.95 | 54.11 | 9 |
| 59.67 | 18.49 | 4 | 105.84 | 27.37 | 6 | 198.49 | 41.08 | 8 | 298.01 | 54.37 | 9 |
| 61.17 | 18.97 | 4 | 107.51 | 27.63 | 6 | 200.68 | 41.39 | 8 | 300.11 | 54.64 | 9 |
| 62.75 | 19.38 | 4 | 109.17 | 27.90 | 6 | 202.88 | 41.71 | 8 | | | |
| 64.36 | 19.80 | 4 | 110.82 | 28.16 | 6 | 205.07 | 42.01 | 8 | | | |
| 65.94 | 20.18 | 4 | 112.51 | 28.41 | 6 | 207.27 | 42.32 | 8 | | | |
| 67.50 | 20.57 | 4 | 114.22 | 28.67 | 6 | 209.51 | 42.64 | 8 | | | |
| 68.29 | 20.87 | 5 | 115.93 | 28.93 | 6 | 211.82 | 42.96 | 8 | | | |
| 69.29 | 20.98 | 5 | 117.63 | 29.19 | 6 | 214.12 | 43.29 | 8 | | | |
| 70.35 | 21.24 | 5 | 119.33 | 29.45 | 6 | 216.42 | 43.59 | 8 | | | |
| 71.44 | 21.49 | 5 | 121.03 | 29.71 | 6 | 218.72 | 43.91 | 8 | | | |

for the decay was applied. Also absorption correction was regarded unnecessary because of the small absorption coefficient $\mu$(= 1.26 mm $^{-1}$). The intensities of 847 independent reflections were obtained by averaging the intensities of equivalent reflections. $R_{int} = 0.019$. The 745 reflections with $I \geq 3\sigma(F_o)$ were used in the subsequent calculation.

### 2.3.1 Crystal Data

$C_5H_{12}Cl_6N_6S_3$, $M_r = 465.1$, trigonal, space group $R\bar{3}c$ (No. 167), $a = 16.049(2)$ Å, $c = 12.412(1)$ Å, $V = 2768.5(6)$ Å$^3$, $Dx = 1.674$ gcm $^{-3}$, $Z = 6$, $\mu = 1.26$ mm $^{-1}$ (Mo $K\alpha$).

### 2.3.2 Structure Determination

The reflection conditions, $-h + k + l = 3n$ for $hkil$; $l = 3n$ for $hh2\bar{h}l$; and $h + l = 3n$, $l = 2n$, for $h\bar{h}0l$, indicate the possible space groups $R3c$ (No. 161) and $R\bar{3}c$ (No.167). The latter was confirmed by a statistical distribution of E values and successful refinement of the structure. The structure was solved by the direct method. In the initial model all the molecules were assumed to be ordered. It was found that C(1) and S(1) atoms of the thiourea molecule lie on the twofold rotation axis and C(2) atom of hexachloroethane molecule on the threefold rotation axis. The centroid of the guest molecule lies on the 32 symmetry point. The position and thermal parameters of the non-hydrogn atoms were refined anisotropically, resulting in reduction of the $R$ value to 0.061.

In the structure of the hexachloroethane molecule thus determined, the C(2)-C(2') and C(2)-Cl(1) bond lengths (1.25 and 1.836 Å) are unusually short and long, respectively, compared with the normal bond lengths. Therefore in the next model the C-C bond was allowed to tilt off from the threefold axis and to intersect it at the center of the C-C bond at the 32 symmetry point. Two models of this type are possible with regard to the relation of the molecular and crystal symmetry elements. In model (i) all atoms of the hexachloroethane molecule are independent of each other with a site occupation factor of 1/6. The guest molecule retains none of its own symmetry elements except the identity element. In model (ii) one of the two C atoms is placed on the c-glide plane with an occupation factor of 1/3 and three of the six Cl atoms of the hexachloroethane placed on general positions. The other carbon atom and three other chlorine atoms are generated by the 32 symmetry operations. In this model the guest molecule has a twofold rotational symmetry by the crystal symmetry operation. In the refinement a restraint was applied to keep the C-Cl and C-C distances at 1.780 and 1.560 Å, respectively, within an estimated error of 0.005 Å. Non-hydrogen atoms except C(2) were refined anisotropically and C(2) isotopically. The $R$ values attained were 0.058 and 0.059 for models (i) and (ii), respectively. There were no significant peaks on the D-Fourier map ($\Delta\rho_{max} = 0.66$ $e$ Å $^{-3}$ and $\Delta\rho_{min} = -0.48$ $e$ Å $^{-3}$). Model (i) gave a slightly smaller $R$ value but we deem the difference insignificant. In fact model (i) has a substantially larger number of variable parameters than model (ii) (78 vs. 48). In model (ii) all the H atoms were located from D-Fourier maps and refined isotropically, to give the final $R$ value of 0.048. We regard model (ii) as representing the actual structure more accurately.

Calculations were carried out with the teXsan

**Table 2** Crystal data, atomic coordinates and equivalent isotropic atomic displacement parameters of (thiourea)$_3$C$_2$Cl$_6$ adduct.

| | |
|---|---|
| Molecular Formula | $[(NH_2)_2CS]_3C_2Cl_6$ |
| Crystal system | Trigonal |
| Space group | $R\bar{3}c$ |
| $a$ / Å | 16.049(2) |
| $c$ / Å | 12.412(1) |
| $\gamma$ / deg | 120 |
| $V$ / Å$^3$ | 2768.5(6) |
| $Z$ | 6 |
| $D_x$ / g cm $^{-3}$ | 1.674 |
| $\mu$ / mm $^{-1}$ | 1.26 (Mo $K\alpha$) |

| Atom | $x$ | $y$ | $z$ | $B_{eq}$ / Å$^2$ |
|---|---|---|---|---|
| S(1) | 0.30366(6) | 0.0 | 0.25 | 2.66(2) |
| C(1) | 0.4103(2) | 0.0 | 0.25 | 2.21(7) |
| N(1) | 0.4464(2) | −0.0111(2) | 0.1591(2) | 3.82(8) |
| Cl(1) | 0.0732(6) | −0.0547(7) | 0.3470(2) | 9.1(2) |
| Cl(2) | −0.1099(5) | −0.0546(7) | 0.3645(10) | 8.2(2) |
| Cl(3) | 0.0734(5) | 0.1282(4) | 0.3467(10) | 4.1(1) |
| C(2) | 0.0088(6) | 0.0044(3) | 0.3105(3) | 12.0(3)* |
| H(1) | 0.416(2) | −0.023(2) | 0.096(2) | 3.9(5)* |
| H(2) | 4.99(2) | −0.010(3) | 0.154(3) | 4.3(5)* |

* $B_{iso}$

$B_{eq} = (8/3)\pi^2[u_{11}(aa^*)^2 + u_{22}(bb^*)^2 + u_{33}(cc^*)^2 + 2u_{12}(aa^*bb^*)\cos\gamma + 2u_{12}(aa^*cc^*)\cos\beta + 2u_{12}(bb^*cc^*)\cos\alpha]$

**Table 3** Anisotropic atomic displacement parameters of (thiourea)$_3C_2Cl_6$.

| Atom | $U_{11}$ /Å$^2$ | $U_{22}$ /Å$^2$ | $U_{33}$ /Å$^2$ | $U_{12}$ /Å$^2$ | $U_{13}$ /Å$^2$ | $U_{23}$ /Å$^2$ |
|---|---|---|---|---|---|---|
| S(1) | 0.0289(4) | 0.0375(6) | 0.0284(4) | 0.0188(3) | −0.0014(2) | −0.0029(4) |
| C(1) | 0.0273(14) | 0.0269(19) | 0.0325(19) | 0.0135(9) | −0.0000(8) | −0.0000(15) |
| N(1) | 0.0374(15) | 0.0579(18) | 0.0379(14) | 0.0300(14) | 0.0021(12) | −0.0038(14) |
| Cl(1) | 0.0708(29) | 0.1569(58) | 0.1000(54) | 0.0869(35) | 0.0063(30) | 0.0420(43) |
| Cl(2) | 0.0359(28) | 0.2001(60) | 0.0693(37) | 0.0372(34) | 0.0139(29) | −0.0082(42) |
| Cl(3) | 0.0749(26) | 0.0294(35) | 0.0717(38) | 0.0060(21) | −0.0221(24) | −0.0051(28) |

**Table 4** Bond distances and angles in (thiourea)$_3C_2Cl_6$.

| | | | |
|---|---|---|---|
| S(1)-C(1) | 1.712(4) | S(1)-C(1)-N(1) | 120.4(2) |
| C(1)-N(1) | 1.330(3) | N(1)-C(1)-N(1') | 119.1(4) |
| Cl(1)-C(2) | 1.777(3) | Cl(1)-Cl(2)-C(2') | 109.4(7) |
| Cl(2)-C(2) | 1.779(4) | Cl(2)-Cl(2)-Cl(27) | 109.3(6) |
| Cl(3)-C(2) | 1.781(4) | Cl(3)-C(2)-C(2') | 102.9(8) |
| C(2)-C(2') | 1.523(9) | Cl(1)-C(2)-Cl(2) | 111.3(5) |
| | | Cl(1)-C(2)-Cl(3) | 111.9(5) |
| | | Cl(2)-C(2)-Cl(3) | 111.7(5) |

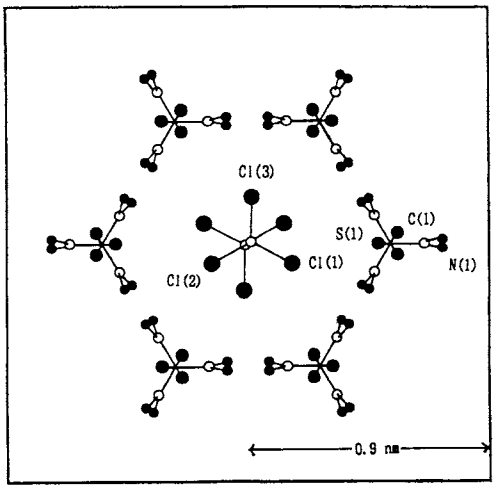


**Fig.3** The crystal structure of thiourea adduct $[(NH_2)_2CS]_3C_2Cl_6$ at 233 K viewed along the c-axis. The guest molecule $C_2Cl_6$ is shown in one of the three equivalent orientations.

structure analysis package (Molecular Structure Corporation, 1985) on a MicroVAXII computer at Graduate School of Science, Osaka University with SHELX76[14] and ORTEPII[15] on an ACOS-S930 computer at Research Center for Protein Engineering, Institute for Protein Research, Osaka University.

**Table 2** lists the final positional and equivalent thermal parameters and their estimated standard deviations. **Table 3** gives the final anisotropic temperature factors with their estimated standard deviations.

## 3. Results and Discussion

### 3.1 Crystal Structure

**Table 4** lists the bond lengths and angles. The perspective view of one channel of the clathrate structure is given in **Fig.3**. Only one of the three orientations of the guest molecule is shown for the sake of clarity. The guest molecule with twofold rotation symmetry perpendicular to the C-C bond is threefold disordered. The C(2)-C(2') bond and the threefold rotation axis intersect each other at an angle of 10.4°.

As shown in **Fig.4**, the thiourea molecules are hydrogen-bonded to one another to build up the channels. The N···S hydrogen bond distances are 3.439 Å in the chains in which thiourea molecules are related by the threefold screw axis, and 3.385 Å between the chains. The thiourea molecules are exactly planar. The three S-C bonds are directed to the centroid of the guest molecule at 120° to each other. The shortest distance between the thiourea S(1) and the guest C(2) atom is 4.755 Å. The bond distance of S(1)-C(1) 1.717(4) Å is shorter, and that of C(1)-N(1) 1.331(3) Å longer than the corresponding distances 1.772 and 1.324 Å in thiourea-adamantane[16] and those (1.727 and 1.322 Å) in thiourea-$CCl_4$[17].

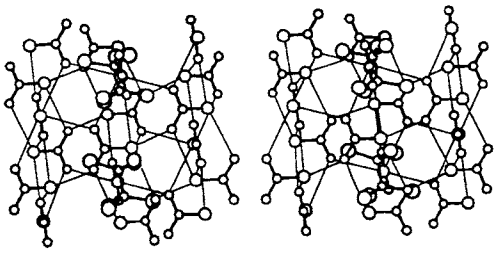

**Fig.4** The crystal structure of thiourea adduct $[(NH_2)_2 \cdot CS]_3C_2Cl_6$ at 233 K in a stereo pair, viewed perpendicular to the c-axis. The guest molecules are recognized in the channel. The y-shaped molecules connected by lines represent the host thiourea of which the hydrogen atoms are not shown. The lines stand for N···S hydrogen bonds.

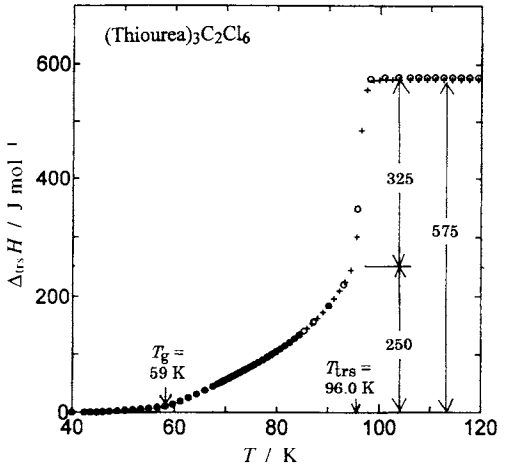


**Fig.5** The enthalpy of transition of $[(NH_2)_2CS]_3C_2Cl_6$.

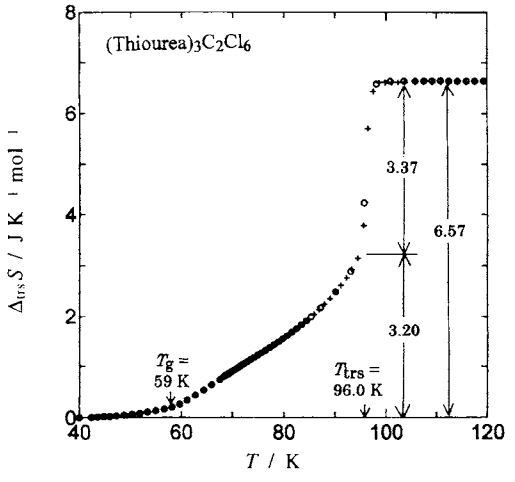


**Fig.6** The entropy of transition of $[(NH_2)_2CS]_3C_2Cl_6$.

As stated in the experimental section, the distinction between the three-fold and six-fold disordered models is marginal in terms of the *R* factor. Also, we had to use chemical restraint in the refinement to attain the reasonable convergence. The heavy disorder of the strong scatterers (Cl atoms) appears to be responsible for the difficulty. In order to attain a more definite result, we are planning to collect the diffraction data at 100 K where the high temperature phase is still stable. It is expected that the thermal motion will be much reduced below the level in the present experiment performed at 233 K and will give a clearer picture of the disordered configuration.

The crystal shattered at the phase transition at 96 K and the structure of the low temperature phase could not be determined. An attempt was made to analyze the powder pattern recorded at 83 K with the help of the known structure of a similar compound thiourea 2,3-dimethylbutadiene.[18] But it was not possible to relate the powder patterns of the two structures to each other.

### 3.2 Phase Transition

The peak of the heat capacity at 96 K represents the latent heat effect of a first order transition. There is a gradual increase of the heat capacity below the transition temperature. The transition enthalpy and entropy were calculated to include this part in addition to the main part (the latent heat contribution). The base line of the heat capacity was determined by interpolation of the heat capacities below the glass transition and above the phase transition temperature into the transition region. The enthalpy and entropy thus determined are plotted in **Fig.5** and **Fig.6** as a function of temperature. The temperature, enthalpy and entropy of transition are (96.0 ± 0.5) K, 575 J mol $^{-1}$ and 6.57 J K $^{-1}$ mol $^{-1}$, respectively. The discontinuous parts are 325 J mol $^{-1}$ and 3.37 J K $^{-1}$ mol $^{-1}$. Two series of measurement shown in the figure with different marks were reproducible to 2 %. The uncertainty related with the baseline could be ± 5 % as judged from a different fitting scheme using a combination of the Debye and Einstein functions.

The crystal structure determined at 233 K is to

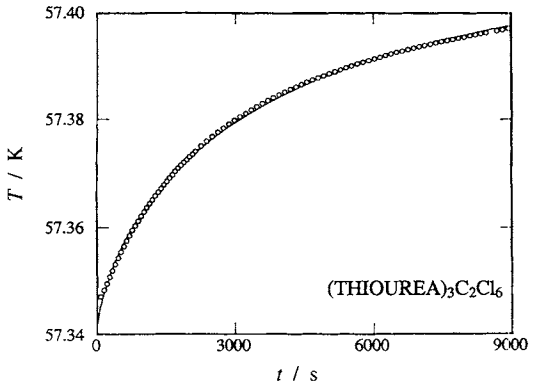


**Fig.7** The spontaneous increase of the temperature of $[(NH_2)_2CS]_3C_2Cl_6$ recorded after rapid cooling from 80 K to 57 K. The best fit exponential curve with $\tau=(4230\pm30)$s is also shown.

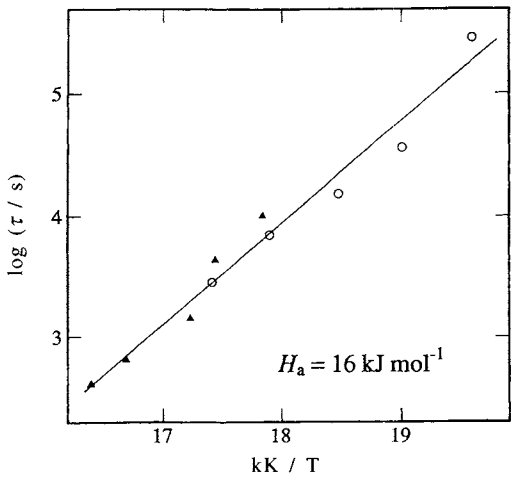


**Fig.8** The Arrhenius plot of the enthalpy relaxation time of $[(NH_2)_2CS]_3C_2Cl_6$ around the glass transition region. The filled triangles were determined by the fitting shown in Fig.7 and similar fitting at different temperatures. The circles represent the data derived by the method described in.[13]

be compared with the high temperature limiting value of the entropy 6.57 J K$^{-1}$ mol$^{-1}$ = $R$ ln 2.2. The disorder in the high temperature phase suggests $R$ ln 3 = 9.13 J K$^{-1}$ mol$^{-1}$. However, the argument requires a closer inspection of the data because of the glass transition at 59 K. Orientational disorder of the guest molecule and its ordering have been discussed for carbon tetrachloride adduct[19,20] and hydrocarbon adducts[4,5] in a closely related way but without participation of the glass transition. Much more extensive disorder has been found in 1,1,2,2-tetrachloroethane adduct by calorimetry.[21]

### 3.3 Glass Transition

In general the relaxation effect is detected by adiabatic calorimetry at the temperature where the enthalpy relaxation time of the substance under study becomes equal to the thermal time constant of the sample cell. There are two methods by which the relaxation time is determined from the temperature drift data![13] Both were used here. In the first, the relaxation time was determined by fitting a relaxation function to the experimental data of the spontaneous temperature increase which the sample experienced when it was cooled from ca. 80 K to ca. 57 K and then kept in thermal isolation. The temperature-time relation was reproduced well by an exponential function of time as shown in **Fig.7**. Similar measurements were performed at different temperatures, giving a set of relaxation times. The second method utilized the temperature drift data from a series of heat capacity determination. By suitably integrating the spontaneous heating rate with time, we determined the relaxation rate as a function of the deviation from the equilibrium. The constant of proportionality between the relaxation rate and the magnitude of the deviation enthalpy from the equilibrium value gives the relaxation time.[13] This method originally devised in 1974 is still useful in the present context, even though the analysis of the relaxation effect has made much progress since that time to include non-linear and non-Arrhenius properties of the glassy state.[22,23] The relaxation times determined by the two methods are plotted in **Fig.8** as a function of reciprocal temperature with different marks. The activation energy 16 kJ mol$^{-1}$ and pre-exponential constant 4.5 ps were derived from the plot. The two sets of data fall on the same straight line if one allows for some scatter of the points. This plot, together with the scanning type of experiment shown in **Fig.2**, establishes the relaxational character of the small heat capacity anomaly at 59 K. We have shown by X-ray diffraction that the guest molecules are disordered over three equivalent orientations in the high temperature phase. It is most likely that the molecules become ordered at the transition point 96 K. The ordering is incomplete in the low temperature phase,

**Table A** The molar incremental standard enthalpy and entropy of (thiourea)$_3C_2Cl_6$ referred to zero kelvin.

| $T$ /K | $C_p/R$ | $\Delta^T_0H/RT$ | $\Delta^T_0S/R$ | $T$ /K | $C_p/R$ | $\Delta^T_0H/RT$ | $\Delta^T_0S/R$ |
|---|---|---|---|---|---|---|---|
| 10 | 1.92 | 0.67 | 1.35 | 170 | 36.98 | 21.97 | 45.27 |
| 20 | 5.41 | 2.17 | 3.97 | 180 | 38.45 | 22.85 | 47.42 |
| 30 | 9.02 | 3.87 | 7.04 | 190 | 39.89 | 23.71 | 49.54 |
| 40 | 12.63 | 5.60 | 10.12 | 200 | 41.33 | 24.55 | 51.62 |
| 50 | 15.76 | 7.29 | 13.24 | 210 | 42.74 | 25.38 | 53.67 |
| 60 | 18.64 | 8.94 | 16.37 | 220 | 44.15 | 26.21 | 55.69 |
| 70 | 21.15 | 10.51 | 19.44 | 230 | 45.53 | 27.02 | 57.69 |
| 80 | 23.43 | 11.98 | 22.41 | 240 | 46.9 | 27.81 | 59.65 |
| 90 | 25.96 | 13.39 | 25.31 | 250 | 48.24 | 28.61 | 61.59 |
| 100 | 26.50 | 15.11 | 28.65 | 260 | 49.57 | 29.39 | 63.51 |
| 110 | 28.02 | 16.21 | 31.25 | 270 | 50.87 | 30.16 | 65.41 |
| 120 | 29.53 | 17.26 | 33.75 | 273.15 | 51.28 | 30.18 | 65.74 |
| 130 | 31.04 | 18.27 | 36.17 | 280 | 52.15 | 30.92 | 67.28 |
| 140 | 32.54 | 19.23 | 38.53 | 290 | 53.41 | 31.67 | 69.13 |
| 150 | 34.03 | 20.17 | 40.82 | 298.15 | 54.41 | 31.96 | 69.92 |
| 160 | 35.51 | 21.08 | 43.07 | 300 | 54.64 | 32.42 | 70.96 |

though most of the disorder is removed discontinuously as is evident from the latent heat of transition. The remaining disorder is removed gradually as the temperature decreases. At the same time the molecule in the channel becomes slower in their reorientational motion as shown in the Arrhenius plot (**Fig.8**). At 56 ~ 58 K the sample falls out of equilibrium during the initial cooling in the calorimetric experiment where the typical time scale is 100 to 1000 s. The relaxation time increases further at lower temperatures, ensuring that the molecules are frozen in the partly disordered state.

We have thus shown that the structural disorder, transition entropy and glass transition are understood consistently by the model allowing three orientations for a guest molecule in the thiourea channel. Interestingly the thiourea carbon tetrachloride clathrate compound is also disordered in the high temperature phase and undergoes ordering phase transitions at low temperature.[19,20] The lowest temperature phase is probably fully ordered in view of the sharp resonance lines of the nuclear quadrupole resonance.[24,25] Also there is no evidence for a glass transition in the carbon tetrachloride adduct. It is likely that a carbon tetrachloride molecule is small enough to reorient in the thiourea channel even below 40 K where the low temperature transition occurs. The thiourea $CCl_3Br$ adduct undergoes two phase transitions at 84 K and 92 K and a glass transition at 20 K.[26] The phase transitions are of the same nature as those in the present adduct and carbon tetrachloride adduct (*i.e.*, related to the orientation of the molecules in the channel). The glass transition in the $CCl_3Br$ adduct arises probably from exchange of the positions of the chlorine and bromine atoms by rotation of the molecule. Thus the glass transition in the present compound is different in its nature from that of the thiourea $CCl_3Br$ adduct.

Finally an interesting problem of the transition temperature remains. The transition temperature 96 K (or equivalently the transition enthalpy 575 J mol $^{-1}$) represents the sum of the interactions between the guest molecules in the same channel and those separated by the wall of the channel. Because the guest molecules are non-polar, long range dipolar interaction is not involved in their ordering as it is in the ordering of the polar guest molecules in hydroquinone clathrate compounds.[1-3] Probably the van der Waals interaction and packing efficiency are playing the major role here to determine the ordering temperatures. As to the barrier against reorientational motion, the potential energy was calculated as a function of the rotation angle of the guest molecule in the channel about the threefold axis assuming additive atom-atom interactions between those belonging to the host and guest molecules. The disorder complicates the

calculation but the average barrier height obtained (13 ~ 16 kJ mol$^{-1}$) agrees well with the experimental activation energy. Considering the structure of the adducts (the same framework accommodating different guest molecules), more elaborate calculation will be of interest for further understanding of their equilibrium and kinetic properties.

**Appendix. The standard thermodynamic functions. Table A**

The increments of standard enthalpy and entropy from zero kelvin were calculated by integration of the heat capacity with temperature using extrapolated values where necessary, and are given in **Table A** in the reduced dimensionless forms. There is an ambiguity in the numerical values arising from the glass transition. If we take the model of disorder from the crystal structure, the incremental standard entropy should be larger than the tabulated values by $R \ln 3 - 6.57$ J K$^{-1}$ mol$^{-1} = 0.308$ $R$ for temperatures above the glass transition. The increase in the standard enthalpy by the same mechanism is indeterminate but is smaller than $0.308\ R \times 59$ K $= 151$ J mol$^{-1}$. By assuming that the correction for the glass transition restores the third law for temperatures higher than $T_g$, one can calculate the Gibbs energy from the tabulated values using the relation $G = H - TS$.

## References


1) T. Matsuo, H. Suga, and S. Seki, *J. Phys. Soc. Jpn.* **22**, 677 (1967).
2) T. Matsuo, *J. Phys. Soc. Jpn.* **30**, 794 (1970).
3) T. Matsuo, H. Suga, and S. Seki, *J. Phys. Soc. Jpn.* **30**, 785 (1971).
4) A. F. G. Cope and N. G. Parsonage, *J. Chem. Thermodyn.* **1**, 99 (1969).
5) A. F. G. Cope, D. J. Gannon, and N. G. Parsonage, *J. Chem. Thermodyn.* **4**, 843 (1972).
6) V. E. Schneider, E. E. Tornau, and A. A. Vlasova, *Chem. Phys. Lett.* **93**, 188 (1982).
7) R. Clement, M. Gourdji, and L. Guibe, *Molec. Phys.* **21**, 247 (1971).
8) S. Hirakawa, T. Imasaka, and T. Matsuo, *J. Phys. Soc. Jpn.* **63**, 593 (1994).
9) J. El. Ghallai, M. Gourdji, L. Guibe, and A. Peneau, *Z. Naturforsch.* **49a**, 433 (1993).
10) H. U. von Lenne, *Acta Crystallogr.* **7**, 1 (1954).
11) G. N. Chekhova, Yu. A. Dyadin, and T. V. Rodionova, *Izv. Sibirskogo Otd. Akad. Nauk SSSR: Ser. Khim. Nauk.* **N5**, 78 (1979).
12) T. Matsuo and H. Suga, *Thermochim. Acta* **88**, 149 (1985).
13) T. Matsuo, M. Oguni, H. Suga, S. Seki, and J. N. Nagle, *Bull. Chem. Soc. Jpn.* **47**, 57 (1974).
14) G. M. Sheldrick, SHELX76. Program for Crystal Structure Determination. University of Cambridge (1976).
15) C. K. Johnson, ORTEPII. Report ORNL-5138. Oakridge National Laboratory, Tennessee, USA.
16) R. Gopal and B. E. Robertson, *Acta Crystallogr.* **C45**, 257 (1989).
17) J. F. Fait, A. Fitzgerald, C. N. Caughlan, and F. P. McCandless, *Acta Crystallogr.* **C47**, 332 (1991).
18) Y. Chatani and S. Nakatani, *Z. Kristallogr.* **144**, 175 (1976).
19) M. Sekii, T. Matsuo, and H. Suga, *J. Incl. Phenom. Molec. Recogn. Chem.* **9**, 243 (1990).
20) K. Yagi, S. Shima, H. Terauchi, and T. Matsuo, *J. Phys. Soc. Jpn.* **66**, 2737 (1997).
21) M. Sekii, T. Matsuo, and H. Suga, *J. Thermal Analysis* **38**, 1861 (1992).
22) H. Fujimori, H. Fujita, and M. Oguni, *Bull. Chem. Soc. Jpn.* **68**, 447 (1995).
23) S. Takahara, O. Yamamuro, and T. Matsuo, *J. Phys. Chem.* **99**, 9589 (1995).
24) T. Matsuo, M. Sekii, N. Nakamura, H. Suga, and H. Chihara, *Z. Natsurforsch.* **45a**, 519(1990).
25) N. Adolphi, M. S. Conradi, and T. Matsuo, *J. Phys. Chem.* **98**, 1968 (1994).
26) T. Matsuo and O. Yamamuro, *Supramolecular Chem.* **6**, 103 (1995).


## 要　旨


ヘキサクロロエタンとチオ尿素からチャンネル型包接化合物を合成し，単結晶X線回折と低温熱容量測定を行った。233 Kにおいて，この化合物は三方晶系に属し，空間群は$R\bar{3}c$であった。構造解析の結果，ゲスト分子はチャンネル中で無秩序配向を取ることがわかった。信頼性因子$R$は0.048であった。熱測定の結果96.0 Kに1次相転移を生じること，および59 Kにガラス転移を生じることが明らかになった。転移エンタルピーは575 J mol$^{-1}$，転移エントロピーは6.57 J K$^{-1}$ mol$^{-1}$であった。このうち不連続部分は325 J mol$^{-1}$と3.37 J K$^{-1}$ mol$^{-1}$であった。転移エントロピーは$R \ln 2.2$に相当する。二つの実験をあわせると，構造解析から導かれた三配向無秩序が相転移で秩序化するが，完全な秩序化にいたる前に分子運動が凍結することが結論される。

以上の結果から，チオ尿素包接格子中におけるゲスト・ゲスト分子間相互作用は物性に顕著な影響を及ぼす大きさをもつことが分った。

松尾隆祐　Takasuke Matsuo
Department of Chemistry, Graduate School of Science, Osaka Univ., TEL. 06-6850-5396, FAX. 06-6850-5397, e-mail: matsuo@chem.sci.osaka-u.ac.jp
研究テーマ：物性物理化学
趣味：英会話，サイクリング

水谷祥之　Yoshiyuki Mizutani
Department of Chemistry, Graduate School of Science, Osaka Univ., 現勤務先；私立名古屋高等学校，TEL. 052-721-5271, FAX. 052-721-6480, e-mail: mizutani@meigaku.ac.jp
趣味：水彩画

菅　宏　Hiroshi Suga
Research Institute for Science and Technology, Kinki Univ., TEL. 06-6721-2332, FAX. 06-6721-2353 e-mail: suga@cc.kindai.ac.jp
研究テーマ：固体の転移現象
趣味：音楽鑑賞

田村初江　Hatsue Tamura
Department of Applied Chemistry, Graduate School of Engineering, Osaka Univ., TEL. 06-6850-5785, FAX. 06-6850-5788, e-mail: tamura@ch.wani.osaka-u.ac.jp
研究テーマ：結晶構造化学
趣味：読書

松林玄悦　Gen-etsu Matsubayashi
Department of Applied Chemistry, Graduate School of Engineering, Osaka Univ., TEL. 06-6850-5785, FAX. 06-6850-5769, e-mail: matsu@ch.wani.osaka-u.ac.jp
研究テーマ：金属錯体集積体の構造と物性
趣味：切手収集，歴史小説